International Journal of Applied Mathematics

Volume 38 No. 8s, 2025

ISSN: 1311-1728 (printed version); ISSN: 1314-8060 (on-line version)

EFFECT PH ON HIBISCUS SABDARIFA DYE IN TIO_2/ SIO_2 NANOCOMPOSITE IN DYE SENSITIZED SOLAR CELLS

Hussein Ali Hussein, Ahmed hassan Abd Almutalb khan, zainab A kadem

Department of Radiological Technologies, College of Health and Medical Technologies, University of Hilla, Babylon, Iraq.

hussein_ali_hussein@hilla-unc.edu.iq

ahmed_abd@hilla-unc.edu.iq

zainb_ahmed@hilla-unc.edu.iq

Abstract

In this study, the titanium dioxide and silicon dioxide nanostructures were prepared by an easy, simple, short time, economic and successful method by mixing with nitric acid diluted .The characterization of the prepared TiO_2 and SiO_2 were studied by field emission scanning (FE-SEM). The optical properties of the prepared nanoparticles TiO_2-SiO_2 by (7-3) molar mass UV-Vis Spectroscopy. The optical band gap of the prepared products is determined by UV-Visible spectrophotometry were found to be(3.3) ev of TiO_2/SiO_2 (7-3) molar mass).

Dye sensitized solar cells were fabricated by using TiO_2/SiO_2 nanocomposite as anode (front electrode) and graphite as cathode (back electrode) deposited on the surface of ITO glass in the presence of hibiscus sabdarifa dye and the electrolyte iodine / iodide solution.

Dye sensitized solar cells depend on pH of dye the DSSCs were fabricated by pH 5.1 is more efficient than other because effect on spectra of dye the extract has a highest but flattened absorption spectrum in the long range wavelength indicating a suppressed absorption peak at this pH and a wider range of red, orange, yellow, and blue light can be absorbed.

Introduction

Nanotechnology provides us with tools to create functional and intelligent materials, devices, and systems by controlling materials in the nano scale, making use of their novel phenomena and associated properties [1].

The band gap (band gap energy) determines the properties of semiconductors by band theory for electrical conductivity [2] . In most of the semiconductors , the band gap energies affected by pH and movement of electrons between the lowest conduction band called lowest occupied molecular orbital (LUMO) and highest valance band , which is called highest occupied molecular orbital (HUMO) [3]. Moreover , the band gap energies for different semiconductors at pH equal zero[4].

Field emission scanning electron microscope is used to examine and analyze the micro-and nanostructured surface morphology. The method is similar to the method of scanning electron

Received: August 06, 2025

Volume 38 No. 8s, 2025

ISSN: 1311-1728 (printed version); ISSN: 1314-8060 (on-line version)

microscope (SEM); however, there is a difference in the electron gun used to scan specimen. In FESEM, a field emission gun is used instead of typical electron gun sources, which provides sharply pointed beam with high electron energy, resulting in minimized charging effects on the specimen and also enhancement of the spatial resolution[5].

Fourier transform infrared spectroscopy (FT-IR) is a physico-chemical method based on vibration analysis of a molecule that is excited by IR radiation at a limited wavelength range [6]. It is used routinely as a method for the representation of various kinds of nanoparticles like metallic NPs and carbon nanomaterials as well as core-shell and hybrid nanoparticles. A variety of publications identify the usage of IR techniques primarily for Fourier transforming infrared spectroscopy (FTIR) to test the functional groups present in a colloidal suspension of NPs [7].

The UV-VIS spectroscopy isi known to be the most effective spectrophotometric technique most commonly used to examine compound varieties. This approach works on calculating electromagnetic radiation interference (EMR) with matters at different wavelength. The UV-VIS spectroscopy includes the fundamentals of UV-VIS spectroscopy, the sources of spectra and the electrical transformation forms. UV-VIS spectroscopy operates well and findings are correct, the components of UV-VIS spectroscopy and their individual role in the proper functioning of a UV-VIS spectrophotometer are very difficult to consider. Light absorption is the basic phenomenon in UV-VIS spectroscopy [8].

A solar cell is a device that converts solar energy into electricity, a clean and vital source of renewable energy, and that can help to overcome the global energy crisis. While commercial solar cells exhibit good performance and durability, there are still many ways to improve solar cell performance and cost through collaborations between scientists, technicians and industrial workers [9]. Solar energy provides an ample amount and free of charge heat and electricity for useful real-life applications. In comparison, unlike non_renewable energy sources, solar energy is environmentally friendly, generating virtually zero emissions. Solar energy is therefore seen worldwide as the most sustainable solution to the energy crisis [10].The operation of a photovoltaic (PV) cell requires 3 basic attributes:

- The absorption of light, generating either electron-hole pairs or exactions.

- The separation of charge carriers of opposite types.

- The separate extraction of those carriers to an external circuit [11].

It is the third generation solar photovoltaic cell that converts the visible light into electrical energy [12] .

Plants have played an important role in the life of human being as they provide the basic need of mankind that is food, clothing, shelter, and medicines. They have formed the basis of traditional medicine system among which are Ayurvedic, Unani etc. that have been in existence for many decades and continue to provide mankind with new remedies. In developing countries, a large section of the population relies on medicinal plants for primary health care requirements. The traditional medicines are becoming popular among most of the world

Volume 38 No. 8s, 2025

ISSN: 1311-1728 (printed version); ISSN: 1314-8060 (on-line version)

population mainly because they are cheap, abundant with less adverse effect on health. In recent years, focus on plant research has increased globally to find out the immense potentials of medicinal plants used in various traditional systems. Various medicinal plants have been studied which could be used as potent phytochemical agents in the therapeutic treatment of various diseases; one among them is Hibiscus sabdariffa known for its delicacy and medicinal properties which has several health benefits [13]. Dye sensitizers are essential to make DSSC function well. It will generate the photon-induced electrons and injecting them into the conducting band of the TiO2 semiconductor [14].

EXPERIMENTALS

Preparation of nono-composit between Titanium dioxide and Silicon dioxide

Take a weight of TiO_2 particles and weight of SiO_2 were acid-treated by stirring in diluted HNO3 solution (10 ml, 0.5 v/v% in deionized water) at 60 °C for 3 h and dried 100 °C for 3 h [15].

Take (FESEM) for the powders of nano-composit

The FESEM is a progressive microscope offering increasing magnification and the ability to observe very fine features at a low voltage than the SEM. This enhances the observation of very fine surface features, electron beam sensitive materials, and non-conductive materials. The FESEM is ideal for imaging polymer materials and thin films[16].

The sample preparation for FESEM is very simple. You have to dispersed nanoparticles then you have to use glass plate/silicon wafer or any solid substrate on which you can keep your nanoparticles containing solution.

Now, dry the nanoparticle containing substrate (glass or wafer) and go for FESEM imaging. If the particles are nonconducting then use gold coat onto the sample containing substrate for very short time (approx. ~30-40 sec). On the other hand, if you have a problem with gold coating then there is a VP (variable pressure) mode option in the FESEM machine, you should try this imaging mode[17].

In this experiment, Roselle was chosen for anthocyanin pigmentation. For the extraction method, the solid-liquid extraction method will be used. First, the dye powder was obtained by heating the Roselle petals via microwave at 60 C^o for two hours. The dried crude is then crushed using mortar and pestle to form a dye powder. This dye dissolved Via ethanol was used to dissolve 20 gm of dye powder. The extracts were heated and stirred using a magnetic stirrer for 10 minutes. The dye extract was then put into the centrifuged machine at the speed of 800 rpm for two minutes to separate any contamination and the extract. The solution was finally filtered to extract anthocyanin [18].

Volume 38 No. 8s, 2025

ISSN: 1311-1728 (printed version); ISSN: 1314-8060 (on-line version)

The working electrodes (WE) consist of a porous layer of metal oxide Semiconductor TiO_2 and SiO_2 conductive glass screen Substrates, per Indium tin oxide (ITO)[19].

The working electrodes were prepared as follows: the saturated Indium tin oxide glass substrates were cleaned with detergent (in order), water and ethanol, TiO_2 and SiO_2 membranes were prepared. Titanium dioxide and Silicon dioxide nanoparticles were dissolved in Nitric acid (diluted) . The glass substrates are heated by burner until the color of semiconductors (white) change to (brown) and return to (white).

A cathode electrode for the DSSC solar cell is prepared from put the indium tin oxide (ITO) glass above the candle and the carbon was formed on glass .

The working electrode is disguised with two-sided duct tape on the area outside the dye. Then, a drop of (0.1M) iodine solution is added in this restricted area. To prepare a (0.1M) iodine solution, an amount of 10g of potassium iodide (KI) is dissolved in 25mL of DIW, and 3.175 g of iodine (I_2), is added, the flask is restopperd until the iodine is completely dissolved and the solution is kept in an opaque bottle[20] then, the counter electrode is placed on the electrode and on the condition that the solution does not leak out of the specified area.

Result and discussion

The Field Emission Scanning Electron Microscope(FESEM) of Titanium dioxide(TiO_2) 7-3 molar mas to SiO_2 .

The FESEM image of TiO_2 (7-3) SiO_2 nanoparticles is shown in Figure 3.2 The particles size is ranged from 60 nm to 80 nm with a heterogeneous spherical shape and rode shape .

Received: August 06, 2025

Volume 38 No. 8s, 2025

ISSN: 1311-1728 (printed version); ISSN: 1314-8060 (on-line version)

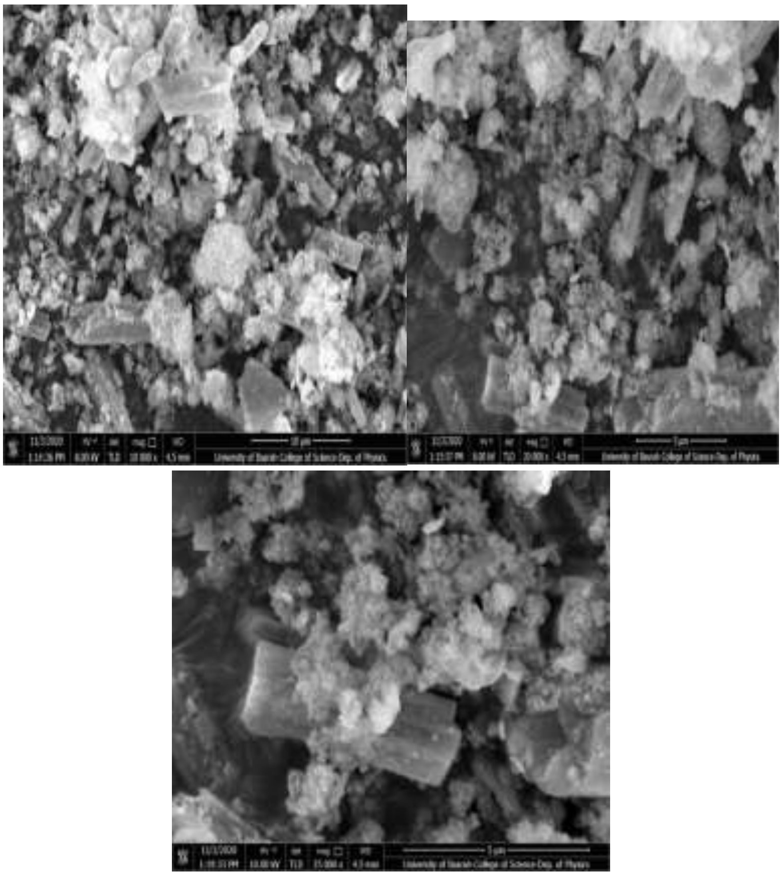

FTIR of SiO_2 nanoparticles , the band around 1057 cm^{-1} corresponds to asymmetric stretching vibration of Si-O-Si band which the bridging oxygen atom moves parallel to the Si-Si lines in the opposite direction to their Si neighbors. The band around 3422 cm^{-1} corresponds to Si-OH stretching vibration, hydrogen bonded [21]. FTIR analysis shows that the silica particles are very hygroscopic in nature. There is also another detected peak at 1635cm^{-1} in the IR spectrum which is attributed to Si-H_2O flexion [22].

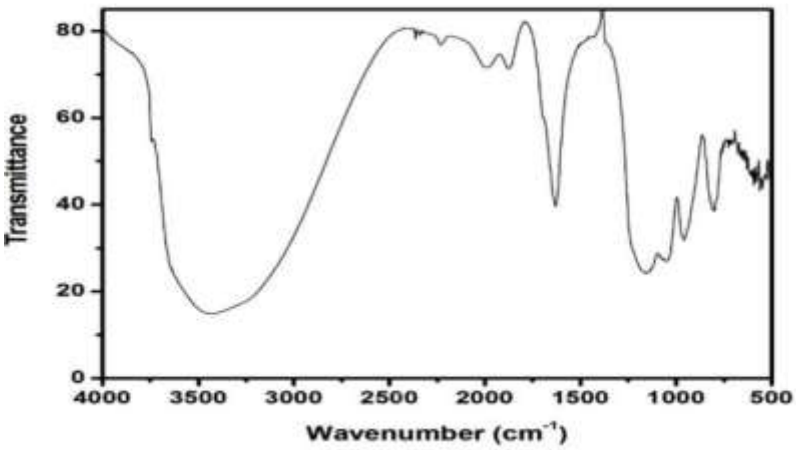

Received: August 06, 2025

Volume 38 No. 8s, 2025

ISSN: 1311-1728 (printed version); ISSN: 1314-8060 (on-line version)

The energy band gap of TiO_2 nanoparticles and TiO_2-SiO_2 composite and SiO_2 nanoparticles calculated from the absorption spectra . Figure(3-9) shows the plot of $(\alpha\ h\upsilon)^2$ verses (hυ) for different nanomaterial . Extrapolating the linear portion of the plot on the axis, the band gap was determined

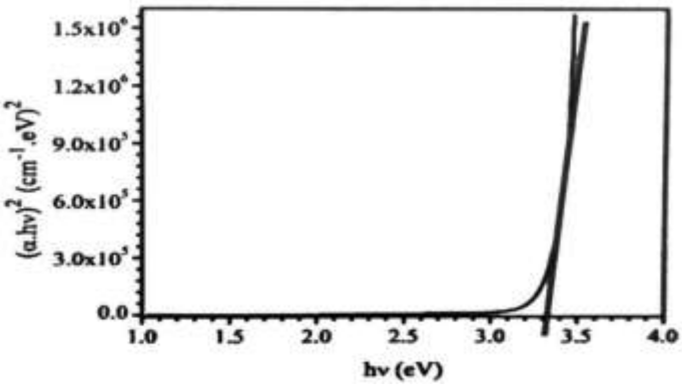

The DSSCs is fabricated using a different value of pH (8.2 , 7.3 , 5.1 , 3.9) on a TiO_2-SiO_2 (7-3) molar mass composite , the figure (3-15) and table (3-8) shown the I and V characteristic of DSSCs of pH (8.2) the result was Voc =800 mV and Isc was 6.8 mA then the (I m) and(V m) (315 mV , 6.1 mA) respectively then the FF is 0.3532 and (Pm) 1.9215 W when we used (1530 mW) intensity of light source the output I and V was (2.2154 mA , 1596 mV) then the η% =2.311.

Value of I (mA) and V (mV) for pH 8.2

m(v)	m(A)
800	0
700	2
600	3.4
500	4.6
400	5.5
300	6.2
200	6.6
100	6.8
0	6.8

International Journal of Applied Mathematics

Volume 38 No. 8s, 2025

ISSN: 1311-1728 (printed version); ISSN: 1314-8060 (on-line version)

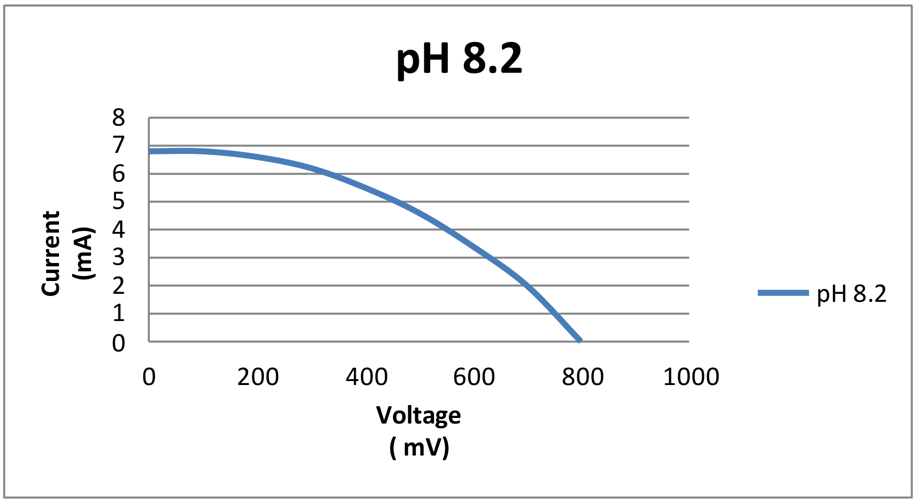

Plot of I (mA) and V (mV) for pH 8.2

The figure (3-16) and table (3-9) shown the I and V characteristic of DSSCs of pH (7.3) the result was Voc =950 mV and Isc was 7.4 mA then the (I m) and(V m) (405 mV , 6.3 mA) respectively then the FF is 0.3629 and (Pm) 2.5515 W when we used (1530 mW) intensity of light source the output I and V was (2.7137 mA , 1635 mV) then the η% =2.9.

Table (3-9) Value of I (mA) and V (mV) for pH 7.3

m(v)	m(A)
950	0
900	1.2
800	2.9
700	4.1
600	4.8
500	5.7
400	6.4
300	6.8
200	7.1
100	7.3
0	7.4

Volume 38 No. 8s, 2025

ISSN: 1311-1728 (printed version); ISSN: 1314-8060 (on-line version)

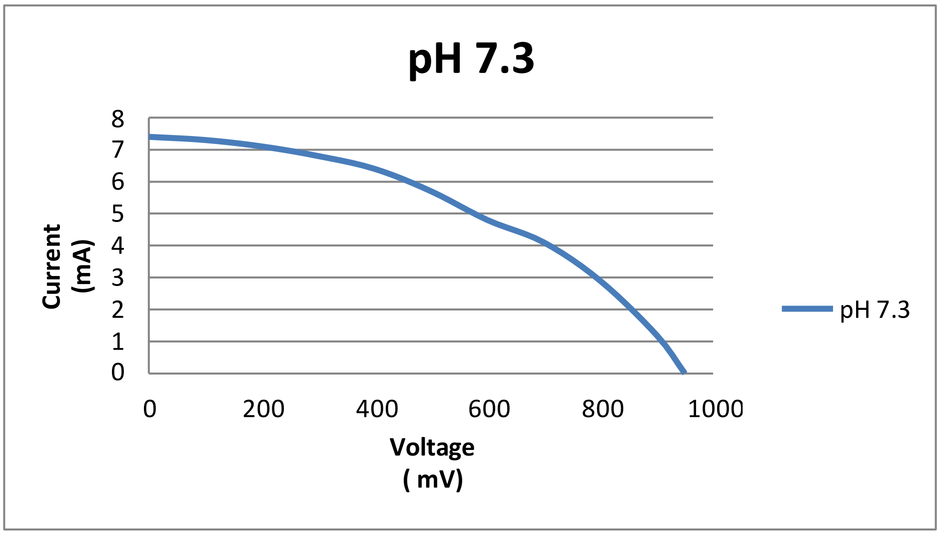

Figure (3-16) Plot of I (mA) and V (mV) for pH 7.3

The figure (3-17) and table (3-10) shown the I and V characteristic of DSSCs of pH (5.1) the result was Voc =1150 mV and Isc was 10.9 mA then the (I m) and(V m) (795 mV , 9.5 mA) respectively then the FF is 0.6025 and (Pm) 7.5525 W when we used (1530 mW) intensity of light source the output I and V was (4.0957 mA , 1715.1 mV) then the η% =4.591.

Table (3-10) Value of I (mA) and V (mV) for pH 5.1

m(v)	m(A)
1150	0
1100	3.5
1000	6.4
900	8.1
800	9.3
700	9.8
600	10
500	10.3
400	10.4
300	10.5
200	10.7
100	10.8
0	10.9

Received: August 06, 2025

International Journal of Applied Mathematics

Volume 38 No. 8s, 2025

ISSN: 1311-1728 (printed version); ISSN: 1314-8060 (on-line version)

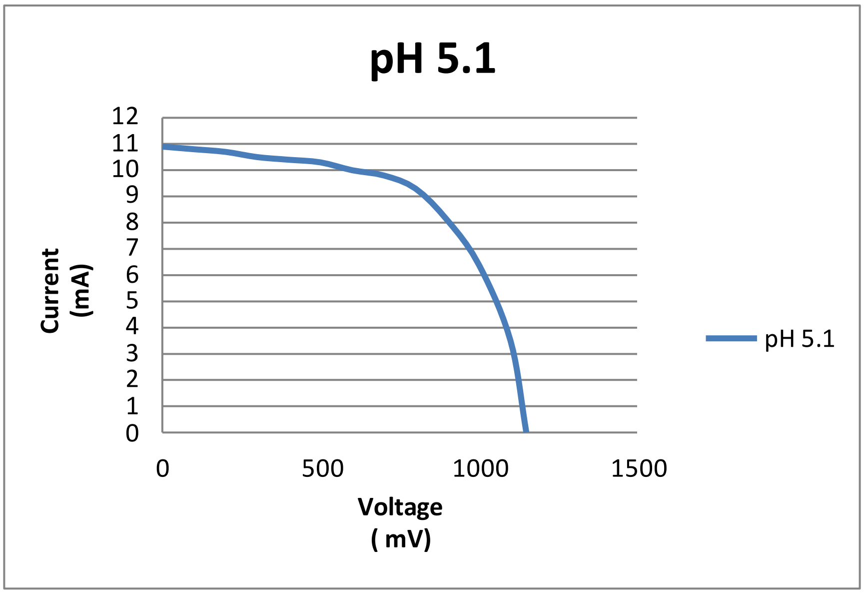

Figure (3-17) Plot of I (mA) and V (mV) for pH 5.1

The figure (3-18) and table (3-11) shown the I and V characteristic of DSSCs of pH (3.9) the result was Voc =1100 mV and Isc was 10.1 mA then the (I m) and(V m) (590 mV , 8.3 mA) respectively then the FF is 0.4407 and (Pm) 4.897 W when we used (1530 mW) intensity of light source the output I and V was (3.9906 mA , 1695 mV) then the η% =4.421 .

Table (3-11) Value of I (mA) and V (mV) for pH 3.9

m(v)	m(A)
1100	0
1000	3.3
900	5.1
800	6.5
700	7.4
600	8.2
500	8.7
400	9.1
300	9.5
200	9.7
100	9.9
0	10.1

Volume 38 No. 8s, 2025

ISSN: 1311-1728 (printed version); ISSN: 1314-8060 (on-line version)

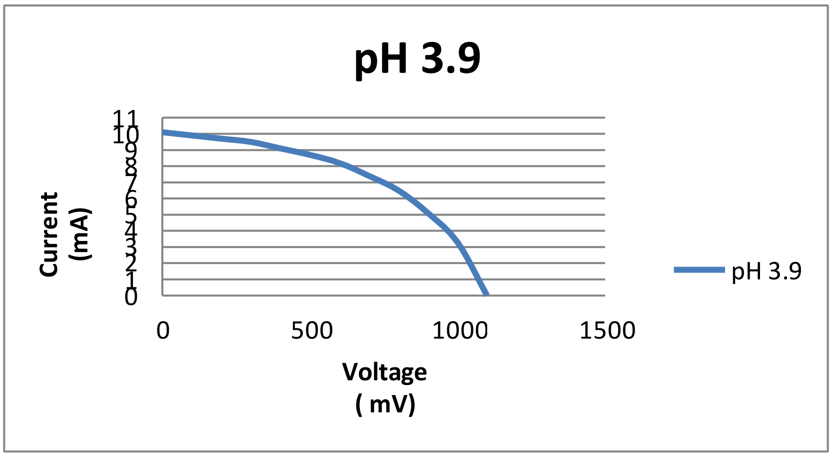

Figure (3-18) Plot of I (mA) and V (mV) for pH 3.9

From the results table (3-12) shown the η% of TiO_2-SiO_2 (7-3) nanocomposite at pH (5.1) is the perfect of dyes had a significant effect on the shape of absorbance spectra . This indicated that the main effectual component on the performance of DSSCs . The pH dependence of absorbance , in acidic conditions, of the anthocyanin form which is capable of more effective coordination to nanocomposite sites [23-26].

At a pH of 5.1 effect on spectra of dye the extract has a highest but flattened absorption spectrum in the long range wavelength indicating a suppressed absorption peak at this pH and a wider range of red, orange, yellow, and blue light can be absorbed [27].

Table (3-12) Photo electrochemical parameters of DSSCs under intensity light (1530 mW)

pH	Isc (mA)	Voc (mV)	I max (mA)	Vmax (mV)	Pmax (W)	FF	η %
2.3	9.5	1000	8.5	525	4.4625	0.4697	4.315
3.9	10.1	1100	8.3	590	4.897	0.4407	4.421
5.1	10.9	1150	9.5	795	7.5525	0.6025	4.591
7.3	7.4	950	6.3	405	2.5515	0.3629	2.9
8.2	6.8	800	6.1	315	1.9215	0.3532	2.311

International Journal of Applied Mathematics

Volume 38 No. 8s, 2025

ISSN: 1311-1728 (printed version); ISSN: 1314-8060 (on-line version)

References

[1] K. Kalantar-Zadeh and B. Fry, Nanotechnology-enabled sensors. LLC, 2008.

[2] A. Eyasu, O. P. Yadav and R. K. Bachheti, " Photocatalytic Degradation of Methyl Orange Dye using Cr-doped ZnS Nanoparticles under Visible Radiation ", International Journal of Chem Tech Research, Vol. 5, pp. 1452-1461, 2013 .

[3] P. Y. Yu and M. Cardona , "Fundamentals of Semiconductors, Physics and Materials Properties ", 4th ed. , Springer, Berlin Germany, CH1, pp. 2-5 , 2010 .

[4] U. I. Gaya, " Heterogeneous photocatalysis using Inorganic Semiconductor Solid " , 1st ed. , Springer Science, Business Media Dordrecht Holand, CH1, pp. 5-17 , 2014 .

[5] S. Hasson, "Porous In x Ga 1- x N for sensing and solar cell applications," 2014.

[6] P. Zarnowiec, L. Lechowicz, G. Czerwonka, and W. Kaca, "Fourier transform infrared spectroscopy (FTIR) as a tool for the identification and differentiation of pathogenic bacteria," Current medicinal chemistry, vol. 22, no. 14, pp. 1710-1718, 2015.

[7] U.sustaining Shaislamov, photocell: H.Kim,Efficient J.M.Yang,solar and energy B. L. conversion Yang, "CuO/ZnO/TiO2 without external photocathodes bias and underfor a self-visible light," International Journal of Hydrogen Energy, vol. 45, no. 11, pp. 6148-6158,2020.

[8]M. S. H. Akash and K. Rehman, "Ultraviolet-Visible (UV-VIS) Spectroscopy," in Essentials of Pharmaceutical Analysis: Springer, 2020, pp. 29-56.

[9] N. Asim, M. Mohammad, and M. Badiei, "Novel Nanomaterials for Solar Cell Devices," in Nanomateria/sfor Green Energy: Elsevier, 2018, pp. 227-277.

[10] H. Liao, Q. Deng, Y. Shen, G. Wang, S. Wang, and Y. Mao, "Theoretical analysis of doping concentration, layer thickness and barrier height effects on BaSi2 based homojunction solar cells toward high efficiency," Solar Energy, vol. 201, pp. 857-865, 2020.

[11] A. M. Bagher, M. M. A. Vahid, and M. Mohsen, "Types of solar cells and application," American Journal of optics and Photonics, vol. 3, no. 5, pp. 94-113, 2015.

[12] S. Bose, V. Soni, and K. Genwa, "Recent advances and future prospects for dye sensitized solar cells: A review," International Journal of Scientific and Research Publications, vol. 5, no. 4, pp. 1-8, 2015.

[13] B.H. Ali, N. Al Wabel, G. Blunden, Phytochemical, pharmacological and toxicological aspects of Hibiscus sabdariffa L: a review, Photother. Vol . 19 ,pp. 369–375, 2005.

[14] Z. Liu et al., "Influence of the binder on the electron transport in the dye-sensitized TiO2 electrode," Thin Solid Films, vol. 484, no. 1–2, pp. 346–351, 2005,

ISSN: 1311-1728 (printed version); ISSN: 1314-8060 (on-line version)

[15] K. H. Park, E. M.Jin, H. B. Gu, S. E. Shim and Ch. K.Hong," Effects of HNO3 treatment of TiO2 nanoparticles on the photovoltaic properties of dye-sensitized solar cells," Materials Letters . vol. 63, pp.2208–2211, 2009.

[16] S. K. Verma et al ., "Green synthesized MgO nanoparticales infer biocompatibility by reducing in vivo molecular nanotoxicity in embryonic zebrafish through argining interaction elicited apoptosis ., " Sci. Total Environ ., vol. 713, p. 136521, 2020.

[17] S. Yousefi and B. Ghasemi, "Precipitator concentration-dependent optostructural properties of MgO nanoparticles fabricated using natural brine,' SN Appl. Sci ., vol. 2, no. 5, 2020.

[18] N. A. Norhisamudin, N. Sabani, M.M. Shamimin, N. Juhari, S. Shaari, M.F. Ahmad and N. Zakaria," The Effect of Different Solvents in Natural Dyes from Roselle (Hibiscus Sabdariffa) and Green Tea Leaves (Camellia Sinensis) for Dye-Sensitized Solar Cell," Journal of Physics: Conference Series, vol. 10, 2020.

[19] Z. Yu, "Liquid Redox Electrolytes for Dye-Sensitized Solar Cells," KTH Royal Institute of Technology, 2012.

[20] M. Halka, S. Smolen, I. Ledwozyw, and S. Wlodzimierz, "Comparison of Effects of Potassium Iodide and Iodosalicylates on the Antioxidant Potential and Iodine Accumulation in Young Tomato Plants," J. Plant Growth Regul ., no. 0123456789, pp. 1-8, 2019.

[21] E. Moncada, R, Quijada and J Retuert," Nanoparticles prepared by the sol–gel method and their use in the formation of nanocomposites with polypropylene," Nanotechnology, vol. 18, pp. 7, 2007.

[22] H. El- Rassy," NMR and IR spectroscopy of silica aerogels with different hydrophobic characteristics," J. Non- Cryst. Sol. Vol. 351, pp.1603-1610, 2005.

[23] N.J. Cherepy, G.P. Smestad, M. Grätzel, J.Z. Zhang, Ultrafast electron injection: Implications for a photoelectrochemical cell utilizing an anthocyanin dye-sensitized TiO2 nanocrystalline electrode, J. Physiol. Chem. B 10 (1997) 9342–9351.

[24] F.J. Heredia, E. M. Francia-Aricha, J.C. Rivas-Gonzalo, I.M. Vicario and C. Santos-Buelga," Chromatic characterization of anthocyanins from red grapes-I. pH effect," Food Chemistry, vol. 63 , pp. 491-498, 1998

[25] G. Calogero, G. Di Marco, S. Caramori, S. Cazzanti, R. Argazzi and C.A. Bignozzi, "Natural dye sensitizer for photoelectrochemical cells, Energy Environ," Sci, vol. 2, pp. 1162-1172, 2009.

[26] T. Fossen, L. Cabrita and O. M. Andersen, "Color and stability of pure anthocyanins influenced by pH including the alkaline region," Food Chem. vol. 63, pp 435–440, 1998.

[27]H.Martı´nez, A. R. Vargas S., Estevez and M. Rodrı´guez,

[28] Khraibet, M. R., & Kadhim, E. J. (2025). Anti-Lung Cancer Activity of the Herbal

Medicinal Plant Cycas revoluta. Hilla University College Journal For Medical Science, 3(2), 25-30.

[29] Kazem, A. J., Jorani, L. E., & Al-Azzawi, A. K. J. (2025). Concept of Marginal Fit Accuracy of a Single Crown Prosthesis Using Conventional Impression Techniques and Intra-Oral Scanner. Hilla University College Journal For Medical Science, 3(2), 63-69.

[30] Mohsin, M. D., & Edan, B. J. (2024). Impact of Physical Activity and Body Size on Serum Level of Anti-Müllerian Hormone in Women in Babylon Province. Hilla University College Journal For Medical Science, 2(2), 49-57.